Hydrotreatment of Sewage Sludge Derived Hydrothermal Liquefaction Biocrude. Part I: Experimental

Barbara Browning, Nuno Batalha, Margarida Costa Gomes, Dorothée Laurenti, Noureddine Lebaz, Christophe Geantet, Melaz Tayakout-Fayolle

Hydrotreatment of Sewage Sludge Derived Hydrothermal Liquefaction Biocrude. Part I: Experimental

Barbara Browning [a], Nuno Batalha[b], Margarida Costa Gomes[c], Dorothée Laurenti[b], Noureddine Lebaz [a], Christophe Geantet [b], Melaz Tayakout-Fayolle [a].*

[a] Univ Lyon, Université Claude Bernard Lyon 1, CNRS, LAGEPP UMR 5007, 43 Boulevard du 11 novembre 1918, F-69100, Villeurbanne, France

[b] Universite Claude Bernard Lyon 1, CNRS, IRCELYON, UMR 5256, Villeurbanne, F-69100

[c]École Normale Supérieure de Lyon and CNRS, Laboratoire de Chimie, 46 allée d'Italie, 69364 Lyon Cedex 7, France.

KEYWORDS: Sewage sludge, Upgrading, GCxGC, Simulated distillation, Size Exclusion Chromatography, Boiling point estimation.

ABSTRACT:

Hydrothermal liquefaction (HTL) has the potential to produce biofuels from waste, such as sewage sludge. However, the biocrude obtained from hydrothermal liquefaction requires further processing to remove heteroatoms, particularly O, N, and S, and achieve the boiling ranges (T_{eb} < 350°C) compatible with standard petroleum-issued fuels. Here, sewage sludge-derived HTL biocrude was upgraded via hydrotreatment (HDT) under batch conditions, 100 bar of hydrogen, and over durations of 0 – 5 h and at 350, 375, and 390°C to allow the study of the upgrading reaction kinetics. The sewage sludge biocrude and the HDT reaction products were fully characterized by a combination of analytical techniques, enabling a fine description of the evolution of products with operating conditions and the construction of a complete description of the upgraded sewage sludge HTL oil reaction product families as carbon number distributions.

As expected, the concentration of heteroatoms in the HDT liquid product decreased progressively with the reaction time and was more significant at 390°C, with 96% of biocrude S and O and 79% of N being removed after 5 h of reaction. The high concentration of N in the liquid product, e.g., 1.4 wt.% at 390 °C and 5 h reaction, was attributed to denitrogenation-resistant compounds, like carbazoles and indoles, still observed in the liquid after HDT reaction. The amount of liquid product in the range of liquid fuels attained the higher yield, i.e., 73 wt.%, under the harshest conditions. The fuel range products were mainly composed of aliphatic, monoaromatic, and diaromatic hydrocarbons, together with indoles, carbazoles, and monoaromatic-nitrogenated compounds, e.g., amines. The significant concentration of nitrogenated compounds in the fuel range suggests that a subsequent HDT stage, mainly focused on denitrogenation, is necessary for the liquid product to be used as a drop-in fuel.

1. Introduction

Today, in France, 800 ktons of sewage sludge (SS) are produced annually, and more than 10 million tons in EU[1,2]. The energetic use of sewage sludge is often addressed with technological pathways such as anaerobic digestion, combustion, pyrolysis, or gasification[3,4]. Considering the cost of a drying stage, hydrothermal methods are economically of great interest since they reduce energy consumption[5,6]. Indeed, hydrothermal liquefaction (HTL) was demonstrated to be a cost-effective and environmentally friendly technology for valorizing SS[7]. Not only does HTL enable the conversion of SS into an energy-dense product, i.e., biocrude, but this technology has also proven effective for recovering essential nutrients, like P, in this stream[8]. Therefore, HTL could contribute to solving the current challenges surrounding SS waste management[9]. However, despite its advantages, HTL technology still faces multiple challenges. For instance, a significant amount of wastewater, which needs to be dealt with, is generated during the process[10]. Similarly, the biocrude produced from HTL needs significant upgrading before it can be used as a fuel[6].

The history of hydrothermal processes has been summarized by D. C. Elliott[11], but key features for sewage sludges were studied in the 70's on the hydrothermal conversion of various biomass at BOM-PERC (Bureau of Mines Pittsburgh Energy Research Center) using H_2O and CO[12], in the 90's demonstration of a 0.5T/day pilot plant[13], and, finally, in the late 90's the introduction of Shell Hydrothermal upgrading Process (HTU®)[14,15]. With time and increasing production, sewage sludges are now considered a renewable energy

source of growing interest, particularly regarding thermochemical conversion methods like HTL[16]. More recent review articles summarize the chemical reactions, and sometimes catalysts, involved and the operating conditions required for improving SS HTL oil yields[7,9]. This is also concomitant with the development of continuous HTL pilot units and close perspectives to industrialization[7,9]. For the purpose of SS HTL energetic valorization, i.e., biocrude production, higher reaction temperatures, typically above 250°C and up to 450°C, are used, and holding times of several minutes (usually between 5 to 60 min). Note that, in softer conditions, thermal hydrolysis (<200°C) is also of commercial interest, with the purpose of pretreating SS prior to anaerobic digestion[17,18]. Depending on the operating conditions, liquid HTL biocrude yield may vary over a wide range (20 to 60%), as illustrated by Das et al.[19]. The SS HTL biocrude is viscous and acidic, contains heteroatoms, particularly N, O, and S, and, consequently must be upgraded to meet conventional fuel compositions.

The SS biocrude composition depends on multiple factors, including the initial composition of the SS, the HTL process conditions, and the extraction solvent used to recover the biocrude (if any)[7,20–23]. For instance, Jahromi et al.[24] hydrotreated SS biocrudes produced with different HTL extraction solvents and, of the solvents tested, found dichloromethane (DCM) gave the best HTL yield but provided a biocrude that was more difficult to upgrade. Similarly, Silva Thomsen et al.[22] demonstrated that the concentration of proteins in SS is directly related to the final concentration of N in the biocrude, which, like with algal HTL biocrudes, poses a challenge during the upgrading to fuels. Indeed, some of the cyclic and aromatic nitrogen-containing compounds present in HTL oils require severe operating conditions, similar to oil refining [25–27]. Consequently, the characterization of the SS biocrude complex mixture is essential to better understand the composition and reactivity

of the biocrude components. Indeed, SS-derived biocrudes have a complex composition with high oxygen and nitrogen content and are distributed in a wide range of Mw[28]. An example of the SS biocrude complex nature is provided by the work of Zimmermann et al.[29], which identified hundreds of oxygenated and nitrogenated compounds (N_1, N_2, and O_xN_x families), including long-chain fatty acids, amides, and other compounds with varying degrees of aromatization (DBE up to 20) and carbon number up to 40. Thus, understanding the conversion pathway of such a complex mixture during the upgrade stage still poses a significant challenge.

Hydrotreatment (HDT), a conventional refining process, is commonly employed in either one or two stages to remove heteroatoms (S, N, O), increase the H/C atomic ratio, and improve the physico-chemical properties of complex liquid bio-sourced streams, like SS biocrude[28,30–32]. For instance, SS biocrude HDT was performed by Heracleous et al.[31,33] and Haider et al.[34] using a two-step continuous process with an initial low-temperature stabilization stage, which removes the most reactive compounds and prevents significant catalyst deactivation during the second harsher HDT stage. In opposition, Subramaniam et al. demonstrated the HDT of SS biocrude to be feasible in a single stage without significant catalyst deactivation, even after 1500 h[30]. In both cases, the authors used Mo-based sulfide catalysts, typically used in refining, which are robust and sulfur-resistant [35]. Understanding the molecular composition of SS HTL oil and its evolution on upgrading is of primary importance for further industrial developments and kinetic modelling. The range products fuel, i.e., bp < 520°C, can be identified and quantified at the molecular stage by comprehensive GC×GC[28,36], while the description of the heaviest fraction composed of heterocyclic molecules of the SS HTL oil and upgraded products is achieved by using FTICR -MS[31,32]. Nonetheless, characterization techniques, such as SEC and NMR, can

be used as an alternative to providing a global image of the biocrude and upgrade products, helping to quantitatively follow the global composition of biocrude and subsequent upgrade products as demonstrated recently by Batalha et al. [36]

In addition to the molecular composition, other properties, such as acidity, density, viscosity, heat value, thermal stability, and lubricity, are also used to evaluate the potential of HDT liquid products to be used as biofuels[37].

The purpose of the present article is to undertake a comprehensive investigation into the evolution of the SS HTL biocrude upgrading products composition during HDT over a wide range of operating conditions, i.e., T=350 °C – 390 °C and reaction time up to 5 h, and to describe, as far as possible, the evolution of product families and the reactions involved. The HTL biocrude and HDT liquid products composition were characterized by GCxGC-TOFMS, GCxGC-FID, ^{13}C-NMR, SEC, SimDist, CHNS-O, as a function of the HDT operating conditions, as well as the density and viscosity. The SEC, SimDist, and GCxGC data were further exploited to extrapolate the HDT liquid products' heavy fraction boiling point outside the SimDist range. Boiling range cuts were defined for each family identified in the GCxGC data, and molar quantities of each boiling range and the average molar mass of the whole hydrotreated liquids were calculated. This representation was validated by comparison with the average molar masses determined independently by the SEC analysis.

2. Material and methods

In this work, a series of experiments was designed to investigate SS-derived biocrude HDT. Sixteen experiments were performed over three temperatures, 350, 375, and 390°C,

and five durations, t0, 30 minutes, 1, 3, and 5 hours. Mass balances were done, and solid, liquid, and gaseous products were analysed with several techniques, as described below.

2.1 Biocrude production

SS from a municipal sewage treatment plant in Rybnik, Poland, stabilized by anaerobic fermentation (physicochemical properties in Table S1) and supplied by PWiK Rybnik was used as the feedstock for the biocrude production. The detailed procedure for producing the biocrude is shown elsewhere[28]. In general, 600 g of slurry containing 10 wt.% of SS in water was heated at 360°C for 30 min under an inert atmosphere in a 1000 mL stainless steel autoclave. After the reaction, the HTL aqueous phase and solid mixture were separated by filtration. Then, the reactor vessel and solid was washed with acetone, and the char and liquid organic fraction (biocrude) solution in acetone were separated by vacuum filtration. The biocrude was recovered after acetone evaporation under rotavap. The biocrude yield was ≈25 wt. %, therefore, the procedure was repeated five times to produce enough biocrude (≈ 75 g) for the work presented in this manuscript. The biocrude from the five experiments was mixed before HDT and characterization.

2.2 Hydrotreatment

2.2.1 Experimental procedure

The HDT of the biocrude was performed under batch conditions using a 300 mL reactor from Parr (Model 4566). The detailed procedure for the catalyst activation, HDT reaction protocol, and product recovery is shown elsewhere[28]. In general, the HDT reaction was performed by using 3 g of biocrude in the presence of 30 g of n-heptane (solvent) and 1 g of NiMoS/Al_2O_3 catalyst (characterization in Table S2). The liquid volume was enough

to cover the stirrer and ensure good mixing. Furthermore, baffles were added to the reactor to improve the mixing of the liquid. It is worth mentioning that the biocrude was not soluble in n-heptane. However, good contact between biocrude and catalyst was still observed due to the lack of char and unconverted biocrude attached to the reactor walls. Additionally, n-heptane is a suitable solvent for HDT reaction products, thus ensuring their recovery. After the reaction, the reactor was cooled to room temperature, and the residual gas was collected in a gas bag and analyzed in a micro-GC (SRA instruments). The liquid and spent catalyst were separated through filtration, and the heptane in the liquid was evaporated in a rotavap for 2 h at a pressure of 30 mbar and a temperature of 40°C. The liquid remaining after evaporation was considered the liquid product from HDT. It is worth mentioning that under reaction conditions, n-heptane is in the supercritical state, which has been demonstrated to enhance HDT by facilitating the supply of H_2 to the catalyst [38–40]. The HDT of the SS biocrude was done at three reaction temperatures, i.e., 350 °C, 375 °C, and 390°C, and reaction times ranging from 30 min to 5 h, leading to a variation of the pseudo-contact time (Equation 1) of 5 to 0.5 h^{-1}.

$$Pseudo\ contact\ time(h^{-1}) = \frac{m_{oil}}{m_{cat}t_{reaction}} \quad \text{Equation 1}$$

Where: m_{oil} and m_{cat} are the mass of biocrude and catalyst, respectively, and $t_{reaction}$ is the reaction time).

2.2.2 Mass balance

The yields of gas (Equation 2), liquid (Equation 3), solid (Equation 4), H_2O (Equation 5), and NH_3 (Equation 6) were determined according to the following equations:

$$Yield_{gas}\ (wt.\%) = \frac{\sum \frac{y_i P_{cold} Mw_i}{(V_{reactor} - V_{heptane}) RT_{ambient}}}{m_{biocrude} + m_{H2}}$$ Equation 2

$$Yield_{liquid}\ (wt.\%) = \frac{m_{liquid}}{m_{biocrude} + m_{H2}}$$ Equation 3

$$Yield_{solid}\ (wt.\%) = \frac{m_{spent\ cat} - m_{cat}}{m_{biocrude} + m_{H2}}$$ Equation 4

$$Yield_{H_2O}\ (wt.\%) = \frac{m_{biocrude} O_{biocrude} - m_{gas} O_{gas} - m_{liquid} O_{liquid}}{m_{biocrude} + m_{H2}} \frac{18}{16}$$ Equation 5

$$Yield_{NH_3}\ (wt.\%) = \frac{m_{biocrude} N_{biocrude} - m_{spent\ cat} N_{spent\ cat} - m_{liquid} N_{liquid}}{m_{biocrude} + m_{H2}} \frac{17}{14}$$ Equation 6

Where: y_i is the compound i gas molar fraction; P_{cold} is the total pressure of the reactor when cold, Mw_i is the molecular weight of the compound i; $V_{reactor}$ is the volume of the reactor (300 mL); $V_{heptane}$ is the volume of heptane; R is the molar gas constant; $T_{ambient}$ is the temperature of the reactor after cooling; $m_{biocrude}$ is the mass of biocrude; m_{H2} is the mass of H_2 put inside the reactor; m_{liquid} is the mass of liquid after heptane evaporation; $m_{spent\ cat}$ is the mass of spent catalyst after drying at room temperature overnight; m_{cat} is the mass of fresh sulfided catalyst used in the reaction; $O_{biocrude}$ and O_{liquid}, are the wt.% of oxygen in the biocrude and liquid, respectively, determined by elemental analysis; O_{gas} is the wt.% oxygen in CO and CO_2; and, $N_{biocrude}$, N_{liquid}, and $N_{spent\ catalyst}$ are the nitrogen composition in wt.% of the biocrude, liquid, and spent catalyst determined by elemental analysis.

2.3 Characterization methods

The gas products were collected in a gas bag and analyzed in a micro-GC (SRA instruments) equipped with three modules: Molsieve 5Å (H_2, CO, CH_4), Hayesep A (CO_2, C_2 hydrocarbons), PLOT Al_2O_3/KCl (C_3-C_4 hydrocarbons).

The carbon, hydrogen, nitrogen, sulfur, and oxygen of the biocrude, HDT liquids, and spent catalyst were obtained on a Thermo Scientific FLASH 2000 Organic Elemental Analyzer (accuracy of ± 0.1 wt.%). The elemental composition of biocrude and the HDT liquid were used to determine the HDT extent of deoxygenation (Equation 5), desulfurization (Equation 6), and denitrogenation (Equation 7).

$$Deoxygenation\ (\%) = \left(1 - \frac{O_{HDT\ liquid}}{O_{\text{biocrude}}}\right).100 \qquad \text{Equation 5}$$

$$Denitrogenation\ (\%) = \left(1 - \frac{N_{HDT\ liquid}}{N_{biocrude}}\right).100 \qquad \textit{Equation 6}$$

The ^{13}C-NMR analysis of the HDT liquids and biocrude was performed in a Bruker AVANCE 400 MHZ spectrometer and analysed using TopSpin 3.0. The measurements were performed at room temperature with an accumulation of 4700 scans for approximately 15 h. The HDT liquid fraction and biocrude (≈100 mg), together with tetramethyl-thiourea (internal standard, 5-10 mg) and chromium acetylacetonate (relaxing agent, 1-3 mg) were diluted in 0.6 mL of deuterated chloroform ($CDCl_3$). Table S3 includes the chemical shifts attributed to each functional group.

The quantification of the hydroxyl groups in the sewage sludge biocrude was performed by quantitative ^{31}P liquid NMR. The detailed experimental procedure and the ^{31}P NMR spectrum for the sewage sludge biocrude are in the supporting material.

The molecular weight distribution of the compounds in the biocrude and HDT liquid products was obtained by size exclusion chromatography (SEC) using an Agilent 1200 series HPLC equipped with two PLgel Columns (50 and 500 Å), a refractive index detector (RID), and a diode array detector (DAD). The analysis was carried out at 35 °C using tetrahydrofuran (THF – 1 mL/min) as eluent. Before analysis, the samples were diluted to a concentration of ≈1 wt.% in THF and filtered (0.45 µm). A mixture composed of linear hydrocarbons with a molecular weight (Mw) comprised between 86 (carbon number = 6) to 1000 (carbon number = 70) g/mol (extrapolated above) was used as the standard to convert elution time into molecular weight (hydrocarbon equivalent - HC).

The boiling point distributions of the HDT liquid products were determined utilizing simulated distillation (Simdis – ASTM 2887) by using an Agilent 7890 gas chromatograph equipped with a flame ionization detector (FID) and a 10 m × 0.53 mm × 0.88 µm ZB-1XT capillary column. The relationship between boiling point and retention time was established using a mixture of linear paraffin with carbon numbers between 6 (Mw = 86 g/mol, bp = 69 °C) and 44 (Mw = 619 g/mol, bp = 545°C). The detected products quantification was made using a standard diesel sample as a reference (initial bp = 114°C and Final bp = 475 °C).

Comprehensive GC×GC-TOFMS, and GC×GC-FID were respectively used to identify and quantify the compounds in the biocrude and HDT liquid. The GC×GC-TOFMS systems were equipped with a cryogenic modulator from Zoex Corporation (USA), as described in Toussaint et al.[41]. The chromatography and TOFMS parameters are described in Table S4. The GC×GC/FID was equipped with a switch valve modulator (Agilent G3486A CFT modulator), and modulation parameters were optimized according to Lelevic et al.[42]. The

parameters used for the analysis are described in Table S4. The compounds detected by GC×GC/FID were quantified using the relative responsive factor method (RRF)[43] with cyclohexanol as reference. The data obtained from comprehensive GCxGC-FID was also used to provide the distillation curve of the HDT of each compound family in the HDT liquid products by using a mixture of n-alkanes (C_7 to C_{40}) as a reference.

The density and viscosity of HTL liquid products were measured at temperatures ranging from 20 °C to 40 °C at intervals of 5 °C using a combined u-shaped vibration-tube density meter and a rolling ball viscosity meter (Anton Paar, model DMA 5000 and Lovis 2000 ME, respectively). The temperature was controlled to 0.001 °C and 0.005 °C and measured with an accuracy better than 0.01 °C and 0.02 °C for the density and viscosity measurements, respectively. A carefully calibrated set of stainless-steel ball and capillary (1.8 mm inner diameter) was used for the viscosity measurements at a fixed angle of 60°. The uncertainty was estimated to be less than 1%. The samples were not degassed prior to analysis. The viscosity was measured using undiluted liquid samples, while the density was measured by diluting the samples (≈40 wt.%) in n-dodecane (time of reaction > 1 h) and acetone (time of reaction < 30 min). The density of the HDT liquid product was calculated by using equation 8.

$$\rho_{HDT\ liquid}\ (\mathrm{g.\,cm^{-3}}) = \frac{\rho_{mixture} - x_{solvent} \cdot \rho_{solvent}}{x_{HDT\ liquid}} \qquad \text{Equation 8}$$

Where: $\rho_{HDT\ liquid}$ is the density of the HDT liquid product ($g.cm^{-3}$); $\rho_{mixture}$ is the density of the diluted HDT liquid product; $x_{solvent}$ and $x_{HDT\ liquid}$ are the respective fractions of solvent, i.e., n-dodecane or acetone in the diluted sample; $\rho_{solvent}$ is the density of the solvent, i.e., n-dodecane or acetone, measured under the same conditions. The

density and viscosity values as a function of temperature can be found in Tables S5 and S6.

3. Results and Discussion

3.1 Biocrude characterization

The physicochemical properties of the SS HTL oil are summarized in Table 1. As expected, the sewage sludge biocrude contains a significant amount of N and O, in the range of 6 wt%, together with a 6500 ppm concentration of S. The nitrogen and sulfur content of the biocrude is compatible with those described in the literature, i.e., N ≈ 4 - 7 wt.% and S ≈ 0.6 – 1.5 wt.%[7]. In contrast, the O content of the biocrude used in this study is lower than those typically reported in the literature, which is typically higher than 10 wt.%, reaching up to 25-30 wt.% in some cases[7]. The low oxygen content observed in the biocrude can be related to the nature of the SS feedstock, which had been submitted to anaerobic digestion before the HTL process. Indeed, Hegdahl et al. performed HTL of anaerobically digested SS with a composition similar to that used in this study and obtained a biocrude with equivalent oxygen content[44]. It is worth mentioning that O concentration is measured experimentally and not determined by difference from the remaining CHNS elements.

The SS biocrude displayed a viscosity of 21.65 Pa.s at 25°C, consistent with values found in the literature for HTL biocrudes produced under similar conditions and after multiple days/months of storage[45]. Thus, the viscosity values suggest some degradation/condensation of the most reactive compounds in the biocrude might have

occurred. This phenomenon could also justify the high biocrude density, i.e., 1.372 g/cm^3 at 25°C, which was higher than the typical values reported in the literature, i.e., $\rho \approx 1$ g/cm^3 [7,31,46].

Table 1. Chemical properties of the biocrude obtained from HTL of SS.

Properties		Functional groups distribution (%, ^{13}C NMR[b])	
C (wt.%)	76.1 ± 0.3	Aliphatic **C**-H, **C**-N	64.0
H (wt.%)	9.7 ± 0.1	Methoxy O-**C**H$_3$	0.7
O (wt.%)	6.2 ± 0.1	Aliphatic **C**-O	3.7
N (wt.%)	6.6 ± 0.1	Aromatic **C**-H	21.0
S (ppm)	6500 ± 11	Aromatic **C**-O, **C**-N	2.1
H_2O (wt.%)	1.0± 0.3	Aromatic **C**-C	5.6
TAN (mg_{KOH}/g)	19.5 ± 1.0	Acid, Ester, Amide (O=**C**-R)	1.9
Total -OH ($mmol/g_{Oil}$)[b]	1.40	Aldehyde and ketone (**C**=O)	1.0
HHV[c] (MJ/kg)	37.3		
Viscosity (25°C, Pa.s)	21.65		
Density (25°C, g/cm^3)	1.372		

[a] ^{13}C NMR spectrum in Figure S2,[b] Quantified by ^{31}P-NMR after phosphytilation with CTMDP.[c] The high heating value (HHV) was determined by using the following expression $HHV\ \left(\frac{MJ}{kg}\right) = 0.3491C + 1.1783H + 0.1005S - 0.1034O - 0.0151N - 0.2011A$, where C, H, S, O, N, and A are the concentrations of carbon, hydrogen, sulfur, oxygen, nitrogen, and ash in wt.%[47].

The carbon functional group composition of the biocrude, determined by ^{13}C NMR, is shown in Table 1 (Spectrum in Ftigurse S1). The most significant contribution is represented by aliphatic C-H and C-N carbon (64.0 %), followed by aromatic C-H (21.0 %). The high occurrence of aliphatic hydrocarbons is expected and typically related to the presence of amides in the biocrude, as observed in the GC×GC/TOF-MS chromatograph in Figure 1. Such compounds in the oil are related to the presence of triglycerides and the respective fatty acids as well as proteins in the parent feedstock[25,28]. According to the GC×GC/TOF-MS, the aromatic carbon in the biocrude was found to be related to the presence of indoles, carbazoles, pyrroles, phenols, and a small amount of aromatic hydrocarbons. It is worth mentioning that the GC×GC data can only account for 30.8 wt.% of the total mass in the biocrude, with the remaining being retained in the column and liner. Indeed, the occurrence of high Mw compounds in the oil can be observed in Figure 2A. Similarly, FTICR-MS analysis of sewage sludge biocrudes made by Heracleous et al. report the presence of compounds with a carbon number up to 45 and varied degrees of aromatization, i.e., DBE up to 20[31].

According to ^{13}C NMR (Table 1) only a small portion of the N and O heteroatoms in the SS biocrude is linked to aromatic carbon. Indeed, most of the N is in the form of amides aliphatic C-N, like amines, while the O is present as amides, carboxylic acids, alcohols, ethers, ketones, and aldehydes. Additionally, the ^{31}P NMR analysis, after phosphitilation of the hydroxyl groups in the SS biocrude showed that 36.1% ($O_{-OH}(\%) = \frac{^{31}P\ NMR-OH.16}{O}$, where ^{31}P NMR-OH is the OH concentration determined in mol/g by ^{31}P NMR and O is the total oxygen concentration in wt.% in the biocrude) of the overall oxygen in the oil belonged to hydroxyl groups, with 17.6% belonging to phenols, 12.7% to carboxylic acids,

and 5.8% to aliphatic alcohols. However, most of the N and O-containing compounds, except for amides, observed via GC×GC/TOF-MS (Figure 1) are part of an aromatic ring or linked to one, suggesting that these compounds are not fully representative of the SS biocrude composition. The FTICR-MS analysis of SS biocrude performed by Heracleous et al. observed that, in the biocrude, N and O-containing compounds were a majority in compounds with low DBE, i.e., 5 – 15[31]. In the same study, the authors observed increased DBE of heteroatom-containing compounds after HDT. Concerning the nature of S in the SS biocrude, no compound was observed in the GC×GC/TOF-MS analysis, suggesting sulfur to be present only in high Mw compounds.

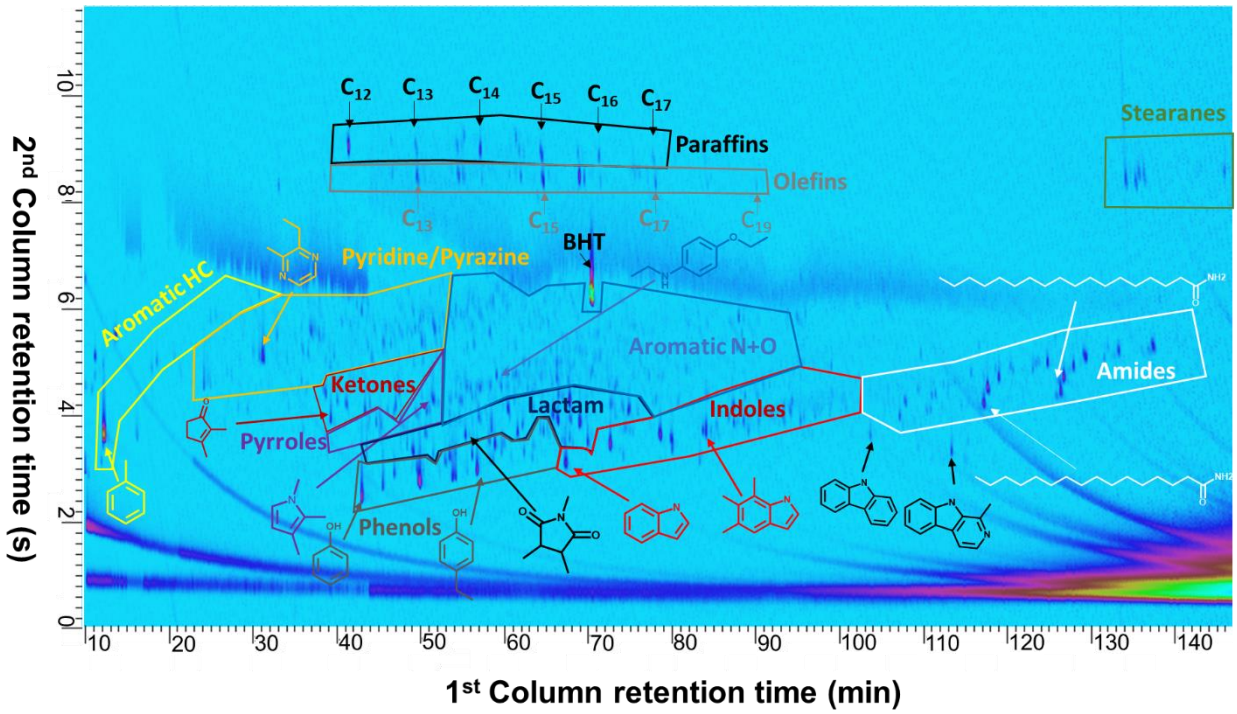

Figure 1. GCxGC/TOF-MS chromatogram of SS HTL biocrude. The quantification of each compound family is in Table S5. BHT = butylated hydroxytoluene (stabilizer present in THF solvent)

3.2 SS biocrude HDT

The SS biocrude was submitted to HDT under different temperatures, i.e., 350 °C, 375 °C, and 390°C, and reaction time, i.e., from 0 h up to 5 h, conditions. The mass balance for the HDT experiments was close to at least 83%, with higher losses for the longer-duration experiments (Figure 2). The missing mass was attributed to three main factors. First, there was an underestimation of gas products. Indeed, the gas yield is calculated by using the residual pressure at room temperature, the empty volume of the reactor, and the concentration of gases determined by µGC (equation 2). Unfortunately, this method considers all gas products to be perfect gases and does not account for the products that are liquid or dissolved in the liquid at the residual pressure and are released as gas when the pressure is released, which leads to an underestimation of the gas yield calculation. Second, the loss of light liquid products during the evaporation of the heptane solvent. Finally, the small biocrude mass used in the study, i.e., 3 g, and, the unavoidable mass losses upon product recovery. The decrease in mass recovered at higher temperatures and reaction times is consistent with the two hypotheses since the yield of gas products and light liquid products is expected to increase under such conditions, as shown in Figure 2 and Figure 4, respectively. Furthermore, the yield of liquid products decreased significantly as the reaction temperature and the reaction time increased. The gas products are primarily composed of light hydrocarbons from C_1 to C_4 (Figure S2). Additionally, CO and small amounts of CO_2 were also observed. The yield of CO and CO_2 did not change significantly wit the reaction conditions, staying between 0.3 wt.% and 0.6 wt.%, indicating most oxygen in the biocrude is removed under the form of H_2O during

the reaction and that the occurrence of decarboxylation and decarbonylation is small. In contrast, the concentration of light hydrocarbons significantly increases with reaction time and temperature and is mainly responsible for the observed variations in the gas yield (Figure 2). The formation of light hydrocarbons can be attributed to the cleavage of larger molecules in the biocrude during the HDT reaction. It is worth mentioning that C-C bound cleavage caused by hydrogenolysis or β-scission is unlikely to occur under the reaction conditions on $NiMoS/Al_2O_3$ catalysts, as discussed in our previous work[36].

At 350 °C, there is a significant amount of solid product yield (27.6 wt.%) at low conversion times, i.e., $t_{reaction}$= 0 h, which decreases as the reaction time increases. A similar, yet less pronounced, evolution is also observed at 375 °C and 390 °C, where the solid yield decreases from ≈ 9-11 wt.%, at $t_{reaction}$ = 0 h to ≈ 6-7 wt.%, after 5 h of reaction. The decrease in solid yield observed at 350 °C is followed by an increase in the liquid yield, suggesting the products to be reactive and most likely composed of heavy molecules, which are transformed into lighter compounds in the liquid range.

The higher concentration of solid products at the start of the reaction ($t_{reaction}$= 0 h) can associated with multiple aspects. First, the reactor is heated under low H_2 (P = 10 bar, T_{room}), with the remaining H_2 (50 bar, $T_{reaction}$) being added once the reaction temperature is attained. This procedure prevents significant condensation of compounds in the oil and subsequent catalyst deactivation by coking. Yet, due to H_2 shortage, condensation reactions should occur faster than HDT and hydrogenation, leading to a high solid yield. Secondly, reactive products in the biocrude are known to undergo condensation at relatively low temperatures, a phenomenon commonly associated with storage problems[45,48]. Thus, condensation of such products, e.g., aldehydes, ketones, alcohols,

etc, is expected to occur during the heating stage. Finally, the higher concentration of solid products at $t_{reaction}$ = 0 h can be related to the poor solubility of polar compounds in n-heptane, which will end up deposited on the catalyst.

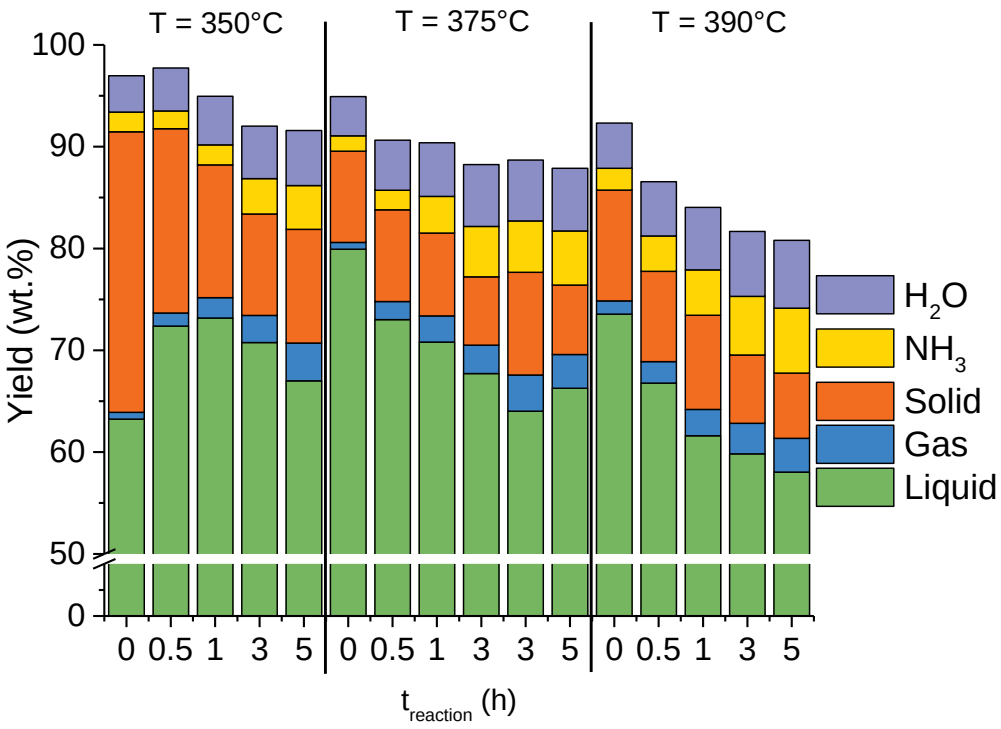

Figure 2. HDT products yield as a function of the reaction temperature (T) and time ($t_{reaction}$). The experimental point at T = 375°C and $t_{reaction}$ =3 h was repeated twice.

The impact of the HDT conditions in deoxygenation (HDO), denitrogenation (HDN), and desulfurization (HDS) are shown in Figure 3. As expected, upgrading reduces the heteroatom content in the products, with higher reaction temperature leading to a higher degree of removal. After 5 h of reaction at 390 °C, 96 % of S and O, and 79 % of N were removed from the liquid product. Indeed, it is well known that HDN is, in general, more difficult to perform when compared to HDO and HDS[27,49,50]. In the specific case of SS

biocrude HDT, Heracleous et al. showed that recalcitrant nitrogenated compounds, such as carbazoles, were formed during the reaction, which resulted in increased resistance to HDN[31]. The increase of HDN and HDO with the reaction temperature and time justifies the increasing formation of H_2O and NH_3 under these conditions (Figure 2).

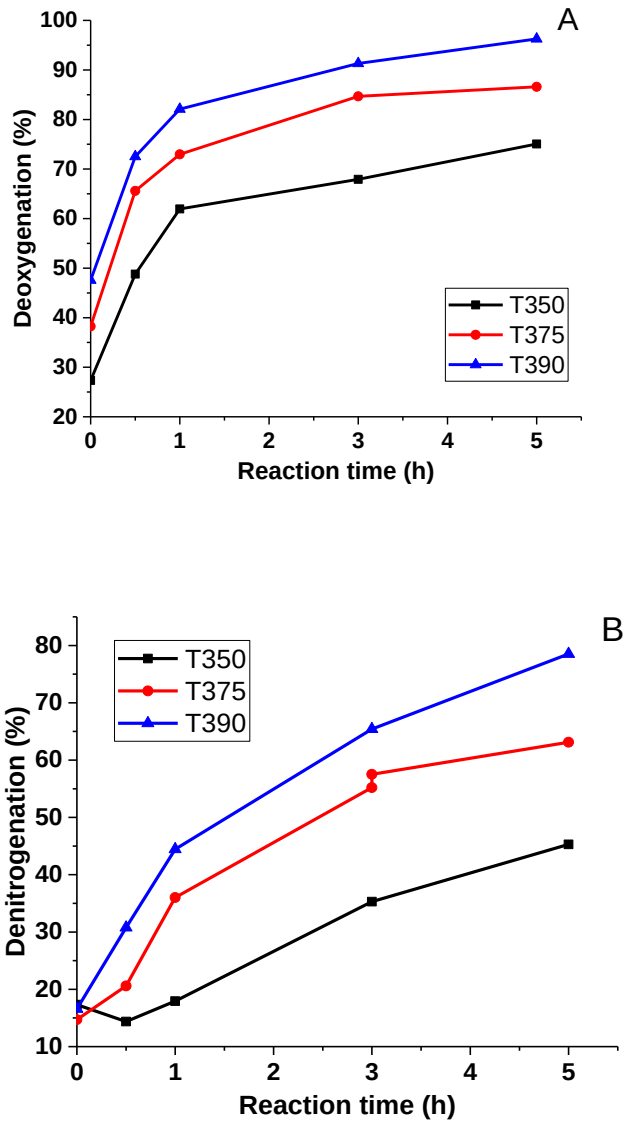

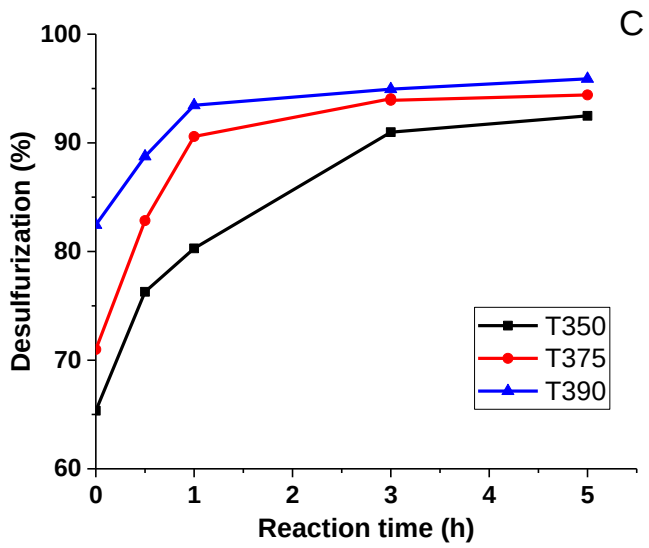

Figure 3. Deoxygenation (A), denitrogenation (B), and desulfurization (C) promoted during the HDT of the SS biocrude as a function of reaction temperature and reaction time. The experimental point at T = 375°C and $t_{reaction}$ =3 h was repeated twice.

The molecular weight (Mw) distribution of the liquid product obtained at 375 °C is shown in Figure 4, with the curves for 350 °C and 390 °C being displayed in supplementary information Figure S3. All compounds in the liquid samples displayed a molecular weight smaller than 1,200 g/mol hydrocarbon equivalent (g/mol_{HC}). When submitted to HDT, there is a clear reduction of the compounds at higher Mw, which are replaced by lighter molecules. Figures 4A and 4B clearly show that the HDT reaction time and reaction temperature contribute to transforming heavier compounds into lighter ones. Thus, the results agree with the hypothesis that the presence of light compound is among the reasons for the lower mass balance closure observed under harsher reaction conditions (Figure 2).

The average Mw of the SS biocrude (260 g/mol_{HC}) was significantly reduced during the HDT (Table S6) until a minimum of 188 g/mol_{HC} at 390 °C and 5 h of reaction time. In addition to the effect of the HDT catalyst on the Mw reduction of the liquid products, a thermal cracking effect was also observed. A significant reduction in Mw was observed after reactor heating, i.e., $t_{reaction}$= 0 h, and the decrease was more significant the higher the reaction temperature used. For instance, when the reaction temperature was 390 °C, the average Mw of the liquid products was 232 g/mol_{HC}, while at 350°C the Mw was 252 g/mol_{HC}. It was also observed that the thermal cracking effect was more significant between 350°C and 375°C than between 375 °C and 390 °C since the average Mw at 375°C was 235 g/mol_{HC}, i.e., much closer to the value observed at 390°C than 350°C. It is worth mentioning that the heating stage took the same time for all temperature conditions, i.e., 20 min, and only a portion of H_2 was present (10 bar).

The significant reduction in Mw observed when comparing the liquid product to the biocrude can also be related to the low solubility of high Mw and polar compounds issued from condensation reactions during heating and not converted from the biocrude in n-heptane. As discussed previously, such products would stay attached to the catalyst and be accounted as solid products, whose yield was quite significant at the beginning of the reaction, i.e., $t_{reaction}$ = 0 h (Figure 2). Upon HDT, such molecules are converted into lower Mw compounds with low polarity and incorporated into the liquid product.

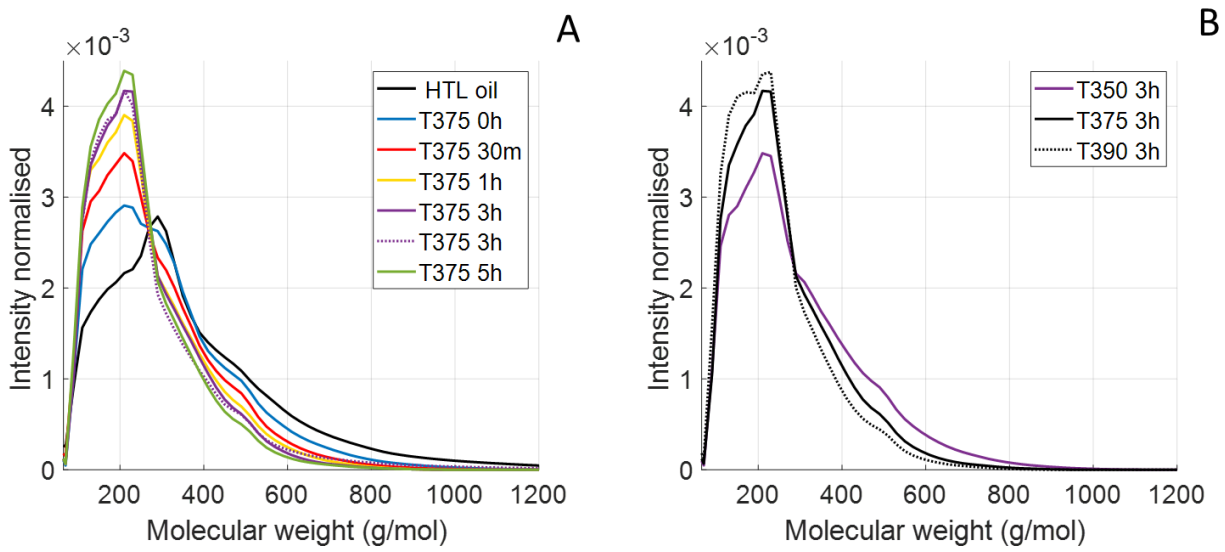

Figure 4. A) Influence of reaction time on the molecular weight distribution (Hydrocarbon equivalent), determined by SEC, of the HDT liquid obtained at 375 °C. B) Influence of reaction temperature on the molecular weight distribution (determined by SEC). The experimental point at T = 375°C and $t_{reaction}$ =3 h was repeated twice.

Figure 5 illustrates the composition of the liquid products, determined by GCxGC/TOF-MS, at the early stages of conversion (Figure 5A, $t_{reaction}$ = 0 h) and after 5 h of reaction (Figure 5B). The quantification of the liquid phase products, performed by GC×GC/FID is shown in Supplementary information Tables S7, S8, and S9. When comparing the chromatograph of the liquid product obtained at $t_{reaction}$ = 0 h and the parent SS biocrude (Figure 1), it is possible to observe a significant increase in aliphatic hydrocarbon products and the appearance of carbazoles. The formation of aliphatic hydrocarbons suggests that some degree of HDT occurs during the heating stage. A significant change in the composition of the liquid phase is observed with the reaction time. As shown in Figure 5B,

after 5 h, the amount of hydrocarbons, including aliphatic, aromatic, and diaromatic hydrocarbons, significantly increases with the reaction time. Additionally, the concentration of oxygenated products, i.e., phenols and aromatic compounds with both nitrogen and oxygen (monoaromatic N+O), significantly decreases, as expected from the reduction in the overall O and N concentration (Figures 2A and 2B).

At high conversion conditions, the nitrogen is mainly in the form of aromatic compounds, such as pyridines, carbazoles, and indoles, which are typically more resistant to HDN[27,51]. For HDN to proceed on such molecules, the hydrogenation of the aromatic ring containing the N atom must occur, followed by cycle opening and N elimination as NH_3[51]. In the specific case of carbazoles, the adjacent ring must also undergo hydrogenation[51,52]. Thus, monoaromatic-N compounds are intermediates in the HDN of indoles and carbazoles into monoaromatic hydrocarbons and naphthenes, which are included in the aliphatic hydrocarbons group (aliphatic hydrocarbons = paraffins + naphthenes). Indeed, the evolution HDO and HDN of aromatic compounds containing heteroatoms is accompanied by the increase in the concentration of monoaromatic compounds, suggesting the latter result from the former conversion (Tables S7, S8, and S9). Aromatic hydrocarbons are further converted into naphthenes (aliphatic hydrocarbons) through hydrogenation, as demonstrated by the continuous decrease of ^{13}C NMR aromatic C-H bounds and increase of aliphatic C-H with the reaction time for all temperatures (Figure S4). Yet, the concentration of aromatic hydrocarbons, detected by GCxGC/FID (Tables S7, S8, and S9) continuously increases with reaction time for all temperature conditions, suggesting that heavy products not visible in GC are being converted into lighter hydrocarbons during HDT, as suggested by SEC analysis (Figure 4)

The aliphatic nitrogenated compounds, such as amides, amines, and nitriles, are no longer part of the liquid products after $t_{reaction}$ = 3 h at 350°C and 375 °C, and $t_{reaction}$ = 1 h at 390 °C. The early conversion of these compounds indicates they undergo HDT quickly. This tendency has also been reported by Heracleaous et al.[31], as well as the fact that residual nitrogen in the liquid product is mainly in aromatic compounds with one or two nitrogen atoms. The presence of nitrile and aliphatic amines was not observed in the parent biocrude, suggesting these compounds are produced during HDT. Zhu et al.[53] studied the HDT amides by using N,N-diethyldodecanamide and N-methyldodecanamide as model compounds and observed that on NiMoS/Al_2O_3 catalysts, the reaction proceeds preferentially through HDO forming a nitrile followed by hydrogenation to amine, and finally HDN to paraffin. Therefore, the observed nitriles and aliphatic amines are intermediate products resulting from the HDT of amides. Additionally, The HDT of amides is also a primary pathway for the production of aliphatic hydrocarbons, in particular paraffins, as opposed to naphthenes resulting from the hydrogenation of aromatic compounds.

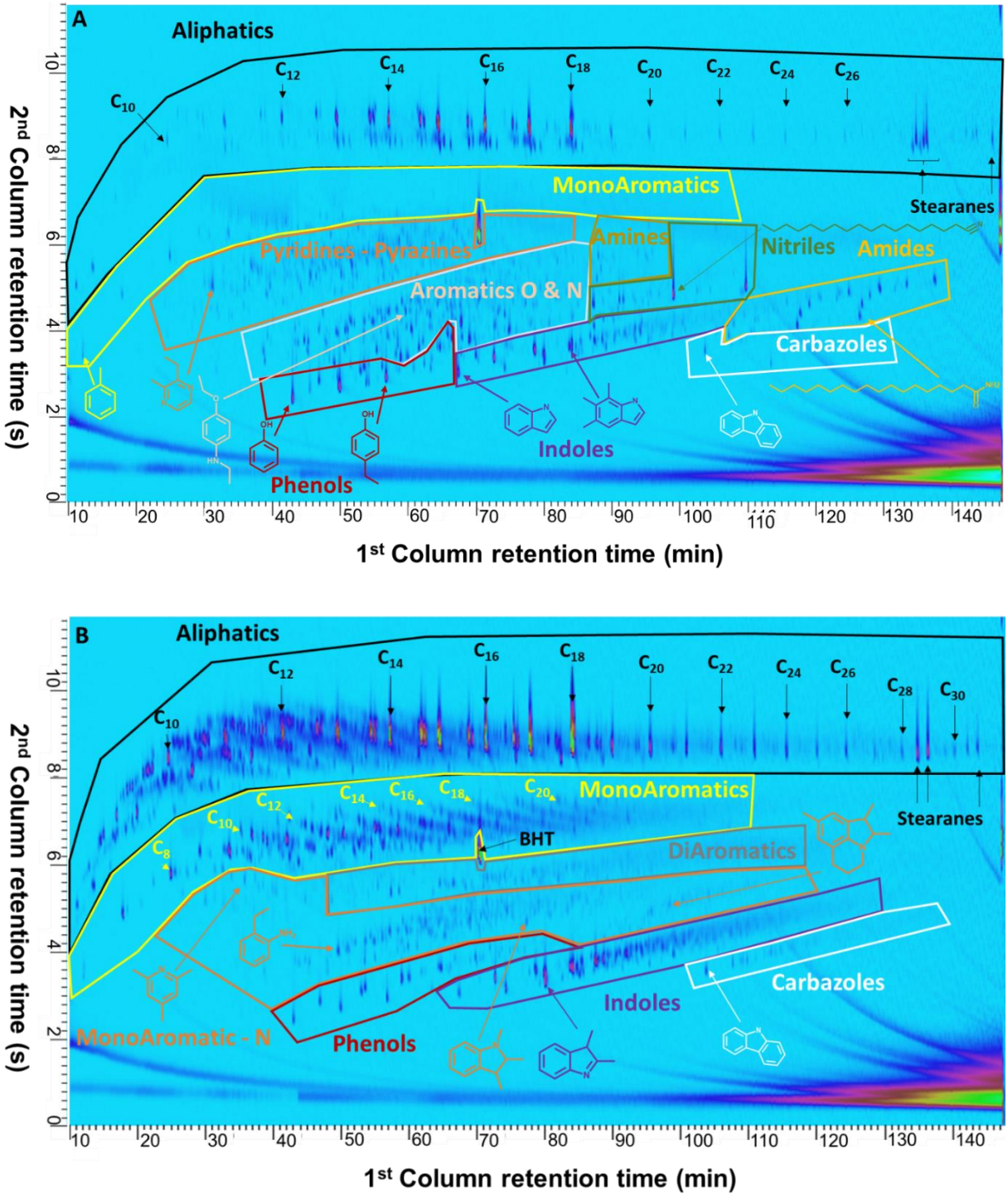

Figure 5. A) GCxGC/TOF-MS chromatogram of HDT liquid product obtained at 375°C after 0 h (A) and 5 h (B) of reaction with product identification according to templates 1 and 2, respectively. BHT = butylated hydroxytoluene (stabilizer present in THF solvent)

The liquid products' density and viscosity are shown in Figures 6A and 6B, respectively. When compared with the parent biocrude, a significant decrease in these two properties can be observed. The high density and viscosity of biocrudes and bio-oils are typically linked to high Mw condensed molecules containing heteroatoms, e.g., N and O, present in their composition [45,48]. Such molecules can be linked to condensation and polymerization reactions occurring during the HTL reaction, which is particularly important when the HTL is performed for longer residence times[5,7]. The occurrence of high Mw components in the biocrude can also be linked to the presence of macromolecules in the parent freedstock[7]. Finally, such molecules can be formed during biocrude storage through the condensation of reactive molecules in the biocrude, e.g., aldehydes and ketones[45,48]. During HDT, the high Mw components and the heteroatoms are removed from the biocrude, as shown in Figures 3 and 4, thus explaining the behavior in HDT liquid viscosity and density observed in Figure 6. It is important to mention that thermal effects also contribute to the reduction of the viscosity and density, as a significant reduction in these parameters can be observed after reactor heating (t = 0 h), where the impact of thermal phenomena is more significant.

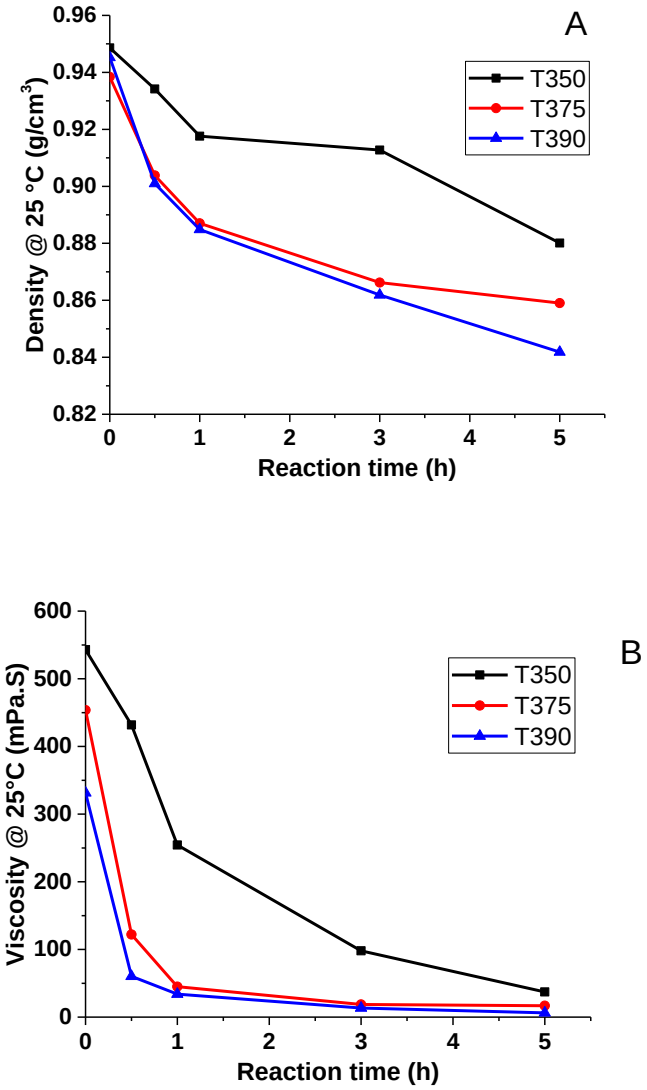

Figure 6. Density (A) and viscosity (B), at 25°C, of the HDT liquid products as a function of reaction temperature and reaction time. Values of density and viscosity between 20°c and 40°C in Tables S10 and S11.

3.3 Correlation between boiling point and molecular weight

This comprehensive analysis allows us to express the evolution during the upgrading of the different compound families. To examine the data, we have differentiated the cumulative boiling curves into 1°C cuts, per Equation 7. This gives the result over the same continuous boiling range as the data.

$\frac{dm_f}{dT_b} = \frac{m_{f,k+1} - m_{f,k}}{T_{b,k+1} - T_{b,k}}$	(7)

$\frac{dm_f}{dT_b}$	Differentiated boiling curve for family, f	g/°C
m	Cumulative mass	g
T_b	Boiling temperature	°C
Subscripts		
f	Family	
k	Data point	

Figure 7 shows an example of a result for experiments performed at 375°C and with durations of 0 h, 1 h, and 5 h. The y-axis is reported in $g.g_{biocrude}^{-1}.°C^{-1}$ because the data is normalised by the mass of biocrude. Amides, aliphatic amines, nitriles, and aromatics + O or N (oxygenated or nitrogenated) are measured only in the early stages of HDT and

have completely disappeared in the longer experiments. The reactor heating time is 20 minutes, and during this period, long-chain fatty acids, commonly found in sewage sludges[31], and assumed to be present initially, have already been consumed. During the reaction period, long-chain amides are converted to their equivalent paraffins via aliphatic amines. Deoxygenation and denitrogenation reactions continue throughout the contact time, with the main final products being aliphatics and monoaromatics. This allows the description of the most important reactions. For instance, there is an important pathway related to the conversion of amides into aliphatics via nitrile and amine intermediates. The other pathways are those usually observed in the HDN of fossil fuels (for instance, pyridine, carbazoles, indols, quinoline denitrogenation[54]) or the HDO of biomass with phenol-based compounds[55].

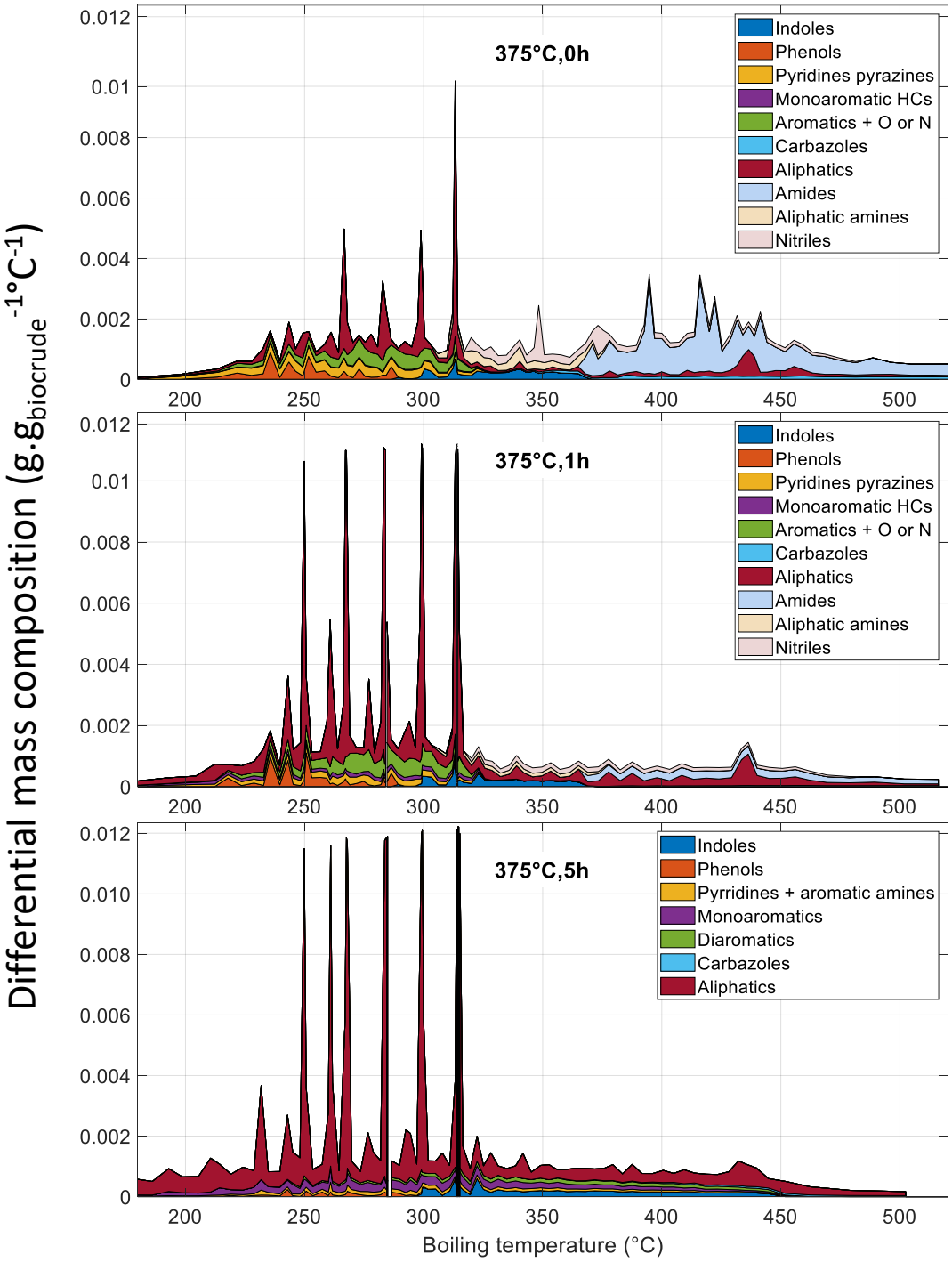

Figure 7. Normalized liquid product quantities from GCxGC/FID in (g.g$_{biocrude}^{-1}$.°C^{-1}), vs boiling point after upgrading at 375°C at t = 0, 1 h, and 5 h.

By using boiling point data, it is also possible to estimate the evolution of the whole liquid product in terms of carbon numbers. For example, Figure 8 shows the evolution of carbon chains of aliphatic compounds during conversion at 350 and 390°C. To cover the complete boiling range, the quantitative SimDist analysis must be extrapolated beyond its maximum boiling point of 530°C. Browning et al. demonstrated that the shape of the GPC curve can be as good as the standard method[56] to extrapolate the boiling curve for heavy oils[57], and so, the same method is applied here, as can be seen in Figure 9. For the feedstock, only about 50 wt% of the liquid could be analyzed and the extrapolation was not attempted. Boiling point estimation was used to relate boiling point to molar mass for all the families present (see supplemental information) and hence obtain quantitative carbon number distributions for each family identified.

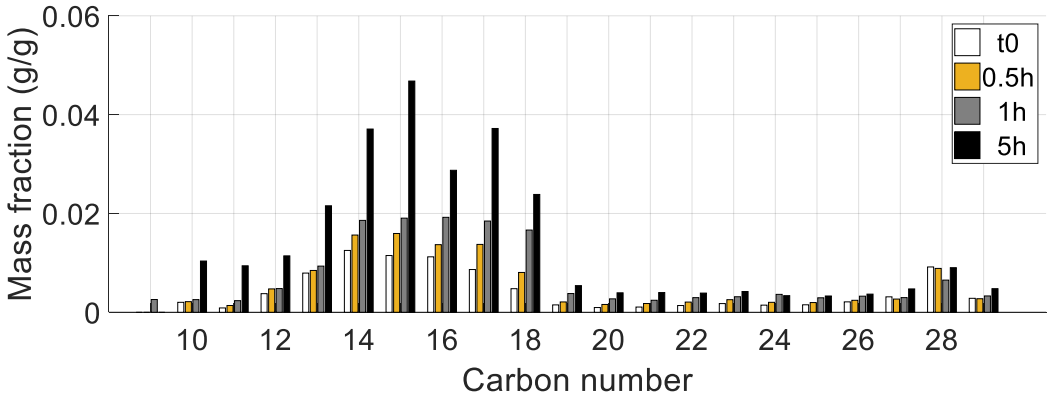

(a)

(b)

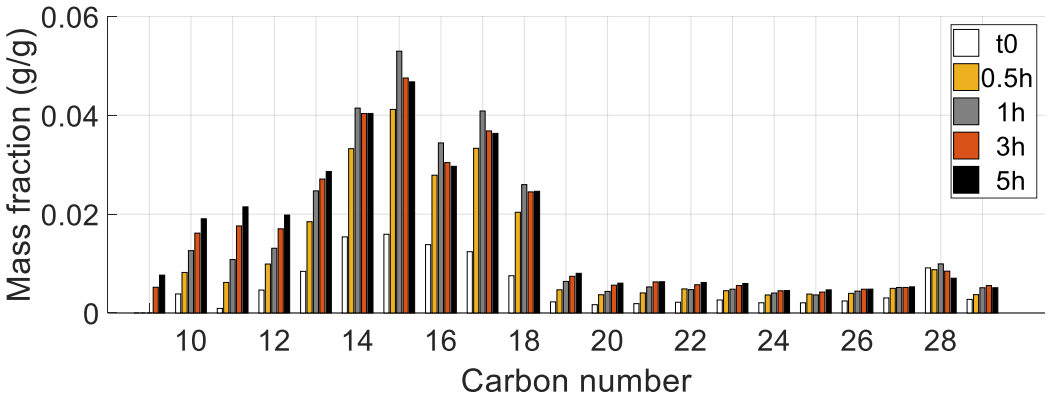

Figure 8. Carbon number distributions for aliphatics at (a) 350°C (b) 390°C.

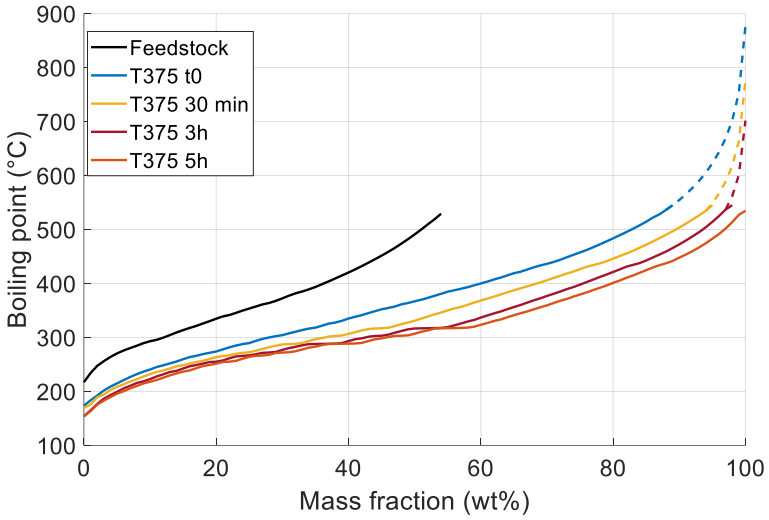

Figure 9. Simulated distillation (SimDist - solid line) with extrapolation (dashed line) of biocrude and HDT liquid product analysis results for experiments at 375°C.

The validity of the method is illustrated by the parity plot obtained in Figure 9. The parity plot compares the calculated average molar mass of each liquid to the measured value from the SEC analysis. The average molar mass, $\overline{M}$, is the sum of all lump masses divided

by the sum of all the molar quantities, as given in Equation **Error! Reference source not found.**(8).

$$\overline{M_m} = \frac{\sum_{i,f} m_{i,f}}{\sum_{i,f} n_{i,f}} \tag{8}$$

The result is close to a linear relationship (coefficient of determination, $R^2 = 0.8716$). This seems reasonable given the assumptions to reduce the complexity of the liquid. The calculated values of $\bar{M}$ are greater than the measured data points, with an average offset of 23.6 g/mol, equivalent to about two C atoms. This is logical because the SEC is calibrated for linear paraffins and the GCxGC column overestimates iso-paraffin boiling points (and hence molar masses) a little due to their slight polarity.

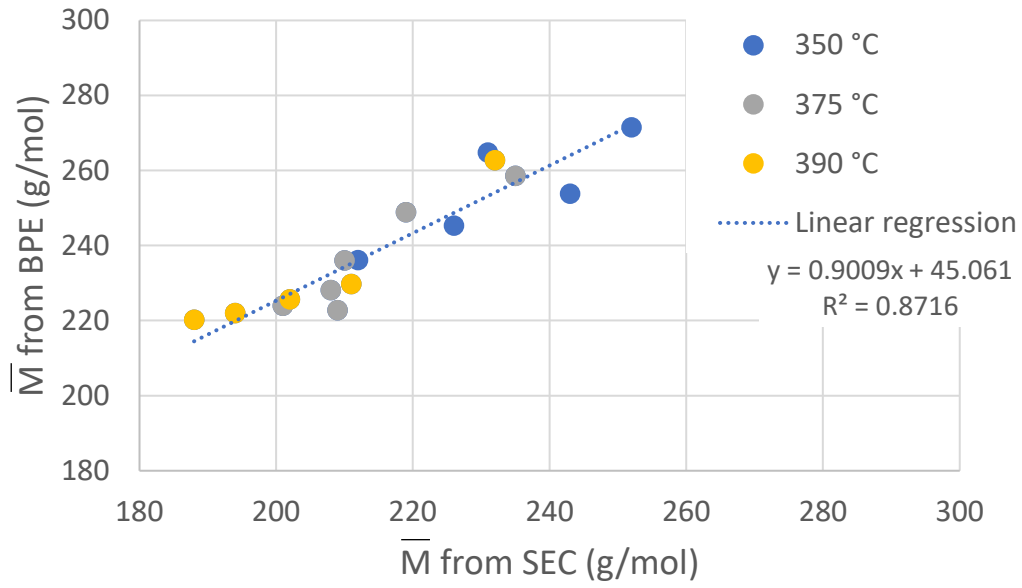

Figure 10. Parity plot for average molar mass ($\overline{M}$) calculated from BPE and measured by SEC analysis.

4. Conclusion

A comprehensive investigation into the evolution of a Sewage Sludge HTL biocrude HDT products composition has been made for a wide range of operating conditions, i.e., T=350 °C – 390 °C and reaction time from 0 to 5 h. The biocrude feedstock was rich in heteroatoms, particularly N (6.6 wt.%) and O (6.2 wt.%), which must be removed for it to be suitable for use as biofuel. The GCxGC analysis of the crude oil revealed a high concentration of amides, phenols, and nitrogenated aromatic compounds, such as indoles, pyrroles, and carbazoles. Furthermore, the biocrude included a significant portion of heavy compounds that were not detectable via GCxGC and that, according to the literature, included a significant degree of heteroatoms, particularly N and O.

After HDT, a significant decrease in the concentration of heteroatoms was observed, and both temperature and reaction time positively influenced the HDT rate. Under the harshest conditions, i.e., 390°C and 5 h of reaction, 96% of biocrude S and O and 79% of N were removed. Still, an N concentration of 1.4 wt.% was observed and attributed to the presence of denitrogenation-resistant compounds, like carbazoles and indoles, still observable in the liquid after HDT reaction.

As the HDT temperature and reaction increased, the concentration of aliphatic hydrocarbon compounds, which were found to originate from the HDT of aliphatic amides and the hydrogenation of aromatic hydrocarbon intermediates, progressively increased. The concentration of aromatic hydrocarbons, particularly mono-aromatic, was also found to increase under harsher HDT conditions. The HDT also promoted a reduction of the overall Mw of the compounds in the liquid due to heteroatom removal and cracking of larger molecules. At 390°C and 5 h of reaction, 73% of the compounds in the liquid phase were in the liquid fuel range, i.e., bp < 350°C, with the fuel range products being composed of aliphatic, monoaromatic, and diaromatic hydrocarbons, together with indoles, carbazoles, and monoaromatic-nitrogenated compounds, e.g., amines. The significant concentration of nitrogenated compounds in the fuel range suggests that a subsequent HDT stage, mainly focused on denitrogenation, is necessary for the liquid product to be used as a drop-in fuel.

The detailed analysis of the composition of HDT liquid products, obtained by GCxGC chromatography, was used together with SEC data to extrapolate the incomplete distillation curve of HDT liquid products. The carbon number distribution representation gives a complete, verified picture of the liquid mass composition for each experiment in

terms of boiling point and molecular structures. It was validated by comparison with the average molar masses determined independently by the SEC analysis and allows for future kinetic modeling of the HDT upgrading reactions.

Hydrothermal liquefaction (HTL) has the potential to produce biofuels from waste, such as sewage sludge. However, the biocrude obtained from hydrothermal liquefaction requires further processing to remove heteroatoms, particularly O, N, and S, and achieve the boiling ranges (T_{eb} < 350°C) compatible with standard petroleum-issued fuels. Here, sewage sludge-derived HTL biocrude was upgraded via hydrotreatment (HDT) under batch conditions, 100 bar of hydrogen, and over durations of 0 – 5 h and at 350, 375, and 390°C to allow the study of the upgrading reaction kinetics. The sewage sludge biocrude and the HDT reaction products were fully characterized by a combination of analytical techniques, enabling a fine description of the evolution of products with operating conditions and the construction of a complete description of the upgraded sewage sludge HTL oil reaction product families as carbon number distributions.

As expected, the concentration of heteroatoms in the HDT liquid product decreased progressively with the reaction time and was more significant at 390°C, with 96% of biocrude S and O and 79% of N being removed after 5 h of reaction. The high concentration of N in the liquid product, e.g., 1.4 wt.% at 390 °C and 5 h reaction, was attributed to denitrogenation-resistant compounds, like carbazoles and indoles, still observed in the liquid after HDT reaction. The amount of liquid product in the range of liquid fuels attained the higher yield, i.e., 73 wt.%, under the harshest conditions. The fuel range products were mainly composed of aliphatic, monoaromatic, and diaromatic hydrocarbons, together with indoles, carbazoles, and monoaromatic-nitrogenated compounds, e.g., amines. The significant concentration of nitrogenated compounds in the fuel range suggests that a subsequent HDT stage, mainly focused on denitrogenation, is necessary for the liquid product to be used as a drop-in fuel.

The data were further exploited by combining and extrapolating the analysis results and using boiling point estimation to obtain carbon number distributions for the identified product families.

5. Acknowledgements

The authors would like to thank the European commission Research Fund for coal and Steel for supporting HYCON project (Grant agreement number 899471).

(1) Ministère de la transition écologique et de la sohésion des térritoires. *Connaître l'état de fonctionnement de la Station de Traitement des Eaux Usées (STEU) de ma commune*. https://assainissement.developpement-durable.gouv.fr/.
(2) Anderson, N.; Snaith; Madzharova, G.; Bonfait, J.; Doyle, L.; Godley, A.; Lam, M.; Day, G. *Sewage Sludge and the Circular Economy*; European Environmental Agency, 2021.
(3) Manara, P.; Zabaniotou, A. Towards Sewage Sludge Based Biofuels via Thermochemical Conversion – A Review. *Renewable and Sustainable Energy Reviews* **2012**, *16* (5), 2566–2582. https://doi.org/10.1016/j.rser.2012.01.074.
(4) Gao, N.; Kamran, K.; Quan, C.; Williams, P. T. Thermochemical Conversion of Sewage Sludge: A Critical Review. *Progress in Energy and Combustion Science* **2020**, *79*, 100843. https://doi.org/10.1016/j.pecs.2020.100843.
(5) Fraga, G.; Batalha, N.; Kumar, A.; Bhaskar, T.; Konarova, M.; Perkins, G. Chapter 5 - Advances in Liquefaction for the Production of Hydrocarbon Biofuels. In *Hydrocarbon Biorefinery*; Maity, S. K., Gayen, K., Bhowmick, T. K., Eds.; Elsevier, 2022; pp 127–176. https://doi.org/10.1016/B978-0-12-823306-1.00009-1.
(6) Perkins, G.; Batalha, N.; Kumar, A.; Bhaskar, T.; Konarova, M. Recent Advances in Liquefaction Technologies for Production of Liquid Hydrocarbon Fuels from Biomass and Carbonaceous Wastes. *Renewable and Sustainable Energy Reviews* **2019**, *115*, 109400. https://doi.org/10.1016/j.rser.2019.109400.
(7) Fan, Y.; Hornung, U.; Dahmen, N. Hydrothermal Liquefaction of Sewage Sludge for Biofuel Application: A Review on Fundamentals, Current Challenges and Strategies. *Biomass and Bioenergy* **2022**, *165*, 106570. https://doi.org/10.1016/j.biombioe.2022.106570.
(8) Matayeva, A.; Rasmussen, S. R.; Biller, P. Distribution of Nutrients and Phosphorus Recovery in Hydrothermal Liquefaction of Waste Streams. *Biomass and Bioenergy* **2022**, *156*, 106323. https://doi.org/10.1016/j.biombioe.2021.106323.
(9) Chen, W.-T.; Haque, Md. A.; Lu, T.; Aierzhati, A.; Reimonn, G. A Perspective on Hydrothermal Processing of Sewage Sludge. *Current Opinion in Environmental Science & Health* **2020**, *14*, 63–73. https://doi.org/10.1016/j.coesh.2020.02.008.
(10) Watson, J.; Wang, T.; Si, B.; Chen, W.-T.; Aierzhati, A.; Zhang, Y. Valorization of Hydrothermal Liquefaction Aqueous Phase: Pathways towards Commercial Viability. *Progress in Energy and Combustion Science* **2020**, *77*, 100819. https://doi.org/10.1016/j.pecs.2019.100819.
(11) Elliott, D. C. Historical Developments in Hydroprocessing Bio-Oils. *Energy Fuels* **2007**, *21* (3), 1792–1815. https://doi.org/10.1021/ef070044u.
(12) Appell, H. R. *Converting Organic Wastes to Oil: A Replenishable Energy Source*; US Department of Interior, Bureau of Mines, 1971.
(13) Itoh, S.; Suzuki, A.; Nakamura, T.; Yokoyama, S. Production of Heavy Oil from Sewage Sludge by Direct Thermochemical Liquefaction. *Desalination* **1994**, *98* (1–3), 127–133. https://doi.org/10.1016/0011-9164(94)00137-5.
(14) Naber, J. E.; Goudriaan, F.; van der Waal, S.; Zeevalkink, J. A.; van de Beld, B. The HTU Process for Biomass Liquefaction: R and D Strategy and Potential Business Development; etde_20041445: United Kingdom, 1999; pp 789–795.
(15) *Biomass: A Growth Opportunity in Green Energy and Value-Added Products; Proceedings of the 4th Biomass Conference of the Americas; Oakland, Calif., USA , August 29 - September 2, 1999. 2*; Overend, R. P., Chornet, E., Eds.; Pergamon: Oxford, 1999; Vol. 2.

(16) Liu, H.; Basar, I. A.; Lyczko, N.; Nzihou, A.; Eskicioglu, C. Incorporating Hydrothermal Liquefaction into Wastewater Treatment – Part I: Process Optimization for Energy Recovery and Evaluation of Product Distribution. *Chemical Engineering Journal* **2022**, *449*, 137838. https://doi.org/10.1016/j.cej.2022.137838.
(17) Barber, W. P. F. Thermal Hydrolysis for Sewage Treatment: A Critical Review. *Water Research* **2016**, *104*, 53–71. https://doi.org/10.1016/j.watres.2016.07.069.
(18) Liang, J.; Li, B.; Zhu, L.; Li, R.; Zhang, J.; Shi, X.; Li, X. Hydrothermal Treatment and Biorefinery of Sewage Sludge for Waste Reduction and Production of Fungal Hyphae Fibers and Volatile Fatty Acids. *Journal of Cleaner Production* **2021**, *289*, 125715. https://doi.org/10.1016/j.jclepro.2020.125715.
(19) Das, P.; Khan, S.; AbdulQuadir, M.; Thaher, M.; Waqas, M.; Easa, A.; Attia, E. S. M.; Al-Jabri, H. Energy Recovery and Nutrients Recycling from Municipal Sewage Sludge. *Science of The Total Environment* **2020**, *715*, 136775. https://doi.org/10.1016/j.scitotenv.2020.136775.
(20) Wei, Y.; Xu, D.; Xu, M.; Zheng, P.; Fan, L.; Leng, L.; Kapusta, K. Hydrothermal Liquefaction of Municipal Sludge and Its Products Applications. *Science of The Total Environment* **2024**, *908*, 168177. https://doi.org/10.1016/j.scitotenv.2023.168177.
(21) Watson, J.; Lu, J.; de Souza, R.; Si, B.; Zhang, Y.; Liu, Z. Effects of the Extraction Solvents in Hydrothermal Liquefaction Processes: Biocrude Oil Quality and Energy Conversion Efficiency. *Energy* **2019**, *167*, 189–197. https://doi.org/10.1016/j.energy.2018.11.003.
(22) Silva Thomsen, L. B.; Anastasakis, K.; Biller, P. Hydrothermal Liquefaction Potential of Wastewater Treatment Sludges: Effect of Wastewater Treatment Plant and Sludge Nature on Products Distribution. *Fuel* **2024**, *355*, 129525. https://doi.org/10.1016/j.fuel.2023.129525.
(23) Matayeva, A.; Fasolini, A.; Bianchi, D.; Chiaberge, S.; De Maron, J.; Basile, F. Production of Biocrude from Organic Waste: Influence of Feedstock Composition on Hydrodenitrogenation Reactivity in Biocrude Upgrading. *Fuel* **2023**, *335*, 126981. https://doi.org/10.1016/j.fuel.2022.126981.
(24) Jahromi, H.; Rahman, T.; Roy, P.; Adhikari, S. Hydrotreatment of Solvent-Extracted Biocrude from Hydrothermal Liquefaction of Municipal Sewage Sludge. *Energy Conversion and Management* **2022**, *263*, 115719. https://doi.org/10.1016/j.enconman.2022.115719.
(25) Matricon, L.; Roubaud, A.; Haarlemmer, G.; Geantet, C. The Challenge of Nitrogen Compounds in Hydrothermal Liquefaction of Algae. *The Journal of Supercritical Fluids* **2023**, *196*, 105867. https://doi.org/10.1016/j.supflu.2023.105867.
(26) Zhuang, X.; Huang, Y.; Song, Y.; Zhan, H.; Yin, X.; Wu, C. The Transformation Pathways of Nitrogen in Sewage Sludge during Hydrothermal Treatment. *Bioresource Technology* **2017**, *245*, 463–470. https://doi.org/10.1016/j.biortech.2017.08.195.
(27) Prado, G. H. C.; Rao, Y.; De Klerk, A. Nitrogen Removal from Oil: A Review. *Energy Fuels* **2017**, *31* (1), 14–36. https://doi.org/10.1021/acs.energyfuels.6b02779.
(28) Batalha, N.; Checa, R.; Lorentz, C.; Afanasiev, P.; Stańczyk, K.; Kapusta, K.; Laurenti, D.; Geantet, C. Lignite and Biomass Waste Hydrothermal Liquefaction Crude Upgrading by Hydrotreatment. *Energy Fuels* **2023**, *37* (14), 10506–10520. https://doi.org/10.1021/acs.energyfuels.3c01550.
(29) Zimmermann, J.; Chiaberge, S.; Iversen, S. B.; Raffelt, K.; Dahmen, N. Sequential Extraction and Characterization of Nitrogen Compounds after Hydrothermal Liquefaction of Sewage Sludge. *Energy Fuels* **2022**, *36* (23), 14292–14303. https://doi.org/10.1021/acs.energyfuels.2c02622.

(30) Subramaniam, S.; Santosa, D. M.; Brady, C.; Swita, M.; Ramasamy, K. K.; Thorson, M. R. Extended Catalyst Lifetime Testing for HTL Biocrude Hydrotreating to Produce Fuel Blendstocks from Wet Wastes. *ACS Sustainable Chem. Eng.* **2021**, *9* (38), 12825–12832. https://doi.org/10.1021/acssuschemeng.1c02743.
(31) Heracleous, E.; Vassou, M.; Lappas, A. A.; Rodriguez, J. K.; Chiaberge, S.; Bianchi, D. Understanding the Upgrading of Sewage Sludge-Derived Hydrothermal Liquefaction Biocrude via Advanced Characterization. *Energy Fuels* **2022**, *36* (19), 12010–12020. https://doi.org/10.1021/acs.energyfuels.2c01746.
(32) Jarvis, J. M.; Albrecht, K. O.; Billing, J. M.; Schmidt, A. J.; Hallen, R. T.; Schaub, T. M. Assessment of Hydrotreatment for Hydrothermal Liquefaction Biocrudes from Sewage Sludge, Microalgae, and Pine Feedstocks. *Energy Fuels* **2018**, *32* (8), 8483–8493. https://doi.org/10.1021/acs.energyfuels.8b01445.
(33) Heracleous, E.; Papadopoulou, F.; Lappas, A. A. Continuous Slurry Hydrotreating of Sewage Sludge-Derived Hydrothermal Liquefaction Biocrude on Pilot-Scale: Comparison with Fixed-Bed Reactor Operation. *Fuel Processing Technology* **2024**, *253*, 108006. https://doi.org/10.1016/j.fuproc.2023.108006.
(34) Haider, M. S.; Castello, D.; Rosendahl, L. A. Two-Stage Catalytic Hydrotreatment of Highly Nitrogenous Biocrude from Continuous Hydrothermal Liquefaction: A Rational Design of the Stabilization Stage. *Biomass and Bioenergy* **2020**, *139*, 105658. https://doi.org/10.1016/j.biombioe.2020.105658.
(35) Toulhoat, H.; Raybaud, P. *Catalysis by Transition Metal Sulphides: From Molecular Theory to Industrial Application*; IFP énergie nouvelles publications; Éd. Technip: Paris, 2013.
(36) Batalha, N.; Checa, R.; Lorentz, C.; Afanasiev, P.; Stańczyk, K.; Kapusta, K.; Laurenti, D.; Geantet, C. Hydrocarbon Fuels from Sequential Hydrothermal Liquefaction (HTL) of Lignite and Catalytic Upgrading of Crude Oil. *Energy Fuels* **2024**. https://doi.org/10.1021/acs.energyfuels.3c04312.
(37) ASTM D7566-22 -Standard Specification for Aviation Turbine Fuel Containing Synthesized Hydrocarbons. In *ASTM Volume 05.04: Petroleum Products, Liquid Fuels, And Lubricants (IV): D7412 – D8128*; ASTM, 2023; Vol. 05.04, p 2074.
(38) Fang, X.; Shi, Y.; Wu, K.; Liang, J.; Wu, Y.; Yang, M. Upgrading of Palmitic Acid over MOF Catalysts in Supercritical Fluid of N-Hexane. *RSC Adv.* **2017**, *7* (64), 40581–40590. https://doi.org/10.1039/C7RA07239B.
(39) Xu, C.; Hamilton, S.; Mallik, A.; Ghosh, M. Upgrading of Athabasca Vacuum Tower Bottoms (VTB) in Supercritical Hydrocarbon Solvents with Activated Carbon-Supported Metallic Catalysts. *Energy Fuels* **2007**, *21* (6), 3490–3498. https://doi.org/10.1021/ef700459s.
(40) Wan, H.; Chaudhari, R. V.; Subramaniam, B. Catalytic Hydroprocessing of P-Cresol: Metal, Solvent and Mass-Transfer Effects. *Topics in Catalysis* **2012**, *55* (3), 129–139. https://doi.org/10.1007/s11244-012-9782-6.
(41) Toussaint, G.; Lorentz, C.; Vrinat, M.; Geantet, C. Comprehensive 2D Chromatography with Mass Spectrometry: A Powerful Tool for Following the Hydrotreatment of a Straight Run Gas Oil. *Anal. Methods* **2011**, *3* (12), 2743–2748. https://doi.org/10.1039/C1AY05045A.
(42) Lelevic, A.; Souchon, V.; Geantet, C.; Lorentz, C.; Moreaud, M. Advanced Data Preprocessing for Comprehensive Two-Dimensional Gas Chromatography with Vacuum Ultraviolet Spectroscopy Detection. *Journal of Separation Science* **2021**, *44* (22), 4141–4150. https://doi.org/10.1002/jssc.202100528.

(43) Scanlon, J. T.; Willis, D. E. Calculation of Flame Ionization Detector Relative Response Factors Using the Effective Carbon Number Concept. *Journal of Chromatographic Science* **1985**, *23* (8), 333–340. https://doi.org/10.1093/chromsci/23.8.333.
(44) Hegdahl, S. H.; Ghoreishi, S.; Løhre, C.; Barth, T. Exploring Hydrothermal Liquefaction (HTL) of Digested Sewage Sludge (DSS) at 5.3 L and 0.025 L Bench Scale Using Experimental Design. *Scientific Reports* **2023**, *13* (1), 18806. https://doi.org/10.1038/s41598-023-45957-9.
(45) Palomino, A.; Godoy-Silva, R. D.; Raikova, S.; Chuck, C. J. The Storage Stability of Biocrude Obtained by the Hydrothermal Liquefaction of Microalgae. *Renewable Energy* **2020**, *145*, 1720–1729. https://doi.org/10.1016/j.renene.2019.07.084.
(46) Snowden-Swan, L. J.; Li, S.; Jiang, Y.; Thorson, M. R.; Schmidt, A. J.; Seiple, T. E.; Billing, J. M.; Santosa, D. M.; Hart, T. R.; Fox, S. P.; Cronin, D.; Kallupalayam Ramasamy, K.; Anderson, D. B.; Hallen, R. T.; Fonoll-Almansa, X.; Norton, J. *Wet Waste Hydrothermal Liquefaction and Biocrude Upgrading to Hydrocarbon Fuels: 2021 State of Technology*; United States, 2022. https://doi.org/10.2172/1863608.
(47) Channiwala, S. A.; Parikh, P. P. A Unified Correlation for Estimating HHV of Solid, Liquid and Gaseous Fuels. *Fuel* **2002**, *81* (8), 1051–1063. https://doi.org/10.1016/S0016-2361(01)00131-4.
(48) Diebold, J. P. *A Review of the Chemical and Physical Mechanisms of the Storage Stability of Fast Pyrolysis Bio-Oils*; NREL, 1999. https://www.osti.gov/biblio/753818.
(49) Raje, A. P.; Liaw, S.-J.; Srinivasan, R.; Davis, B. H. Second Row Transition Metal Sulfides for the Hydrotreatment of Coal-Derived Naphtha I. Catalyst Preparation, Characterization and Comparison of Rate of Simultaneous Removal of Total Sulfur, Nitrogen and Oxygen. *Applied Catalysis A: General* **1997**, *150* (2), 297–318. https://doi.org/10.1016/S0926-860X(96)00317-1.
(50) Furimsky, E. Catalytic Hydrodeoxygenation. *Applied Catalysis A: General* **2000**, *199* (2), 147–190. https://doi.org/10.1016/S0926-860X(99)00555-4.
(51) Bello, S. S.; Wang, C.; Zhang, M.; Gao, H.; Han, Z.; Shi, L.; Su, F.; Xu, G. A Review on the Reaction Mechanism of Hydrodesulfurization and Hydrodenitrogenation in Heavy Oil Upgrading. *Energy Fuels* **2021**, *35* (14), 10998–11016. https://doi.org/10.1021/acs.energyfuels.1c01015.
(52) Tominaga, H.; Nagai, M. Reaction Mechanism for Hydrodenitrogenation of Carbazole on Molybdenum Nitride Based on DFT Study. *Applied Catalysis A: General* **2010**, *389* (1), 195–204. https://doi.org/10.1016/j.apcata.2010.09.020.
(53) Zhu, C.; Gutiérrez, O. Y.; Santosa, D. M.; Flake, M.; Weindl, R.; Kutnyakov, I.; Shi, H.; Wang, H. Kinetics of Nitrogen-, Oxygen- and Sulfur-Containing Compounds Hydrotreating during Co-Processing of Bio-Crude with Petroleum Stream. *Applied Catalysis B: Environmental* **2022**, *307*, 121197. https://doi.org/10.1016/j.apcatb.2022.121197.
(54) Nguyen, M.-T.; Pirngruber, G. D.; Chainet, F.; Albrieux, F.; Tayakout-Fayolle, M.; Geantet, C. Molecular-Level Insights into Coker/Straight-Run Gas Oil Hydrodenitrogenation by Fourier Transform Ion Cyclotron Resonance Mass Spectrometry. *Energy Fuels* **2019**, *33* (4), 3034–3046. https://doi.org/10.1021/acs.energyfuels.8b04432.
(55) Bu, Q.; Lei, H.; Zacher, A. H.; Wang, L.; Ren, S.; Liang, J.; Wei, Y.; Liu, Y.; Tang, J.; Zhang, Q.; Ruan, R. A Review of Catalytic Hydrodeoxygenation of Lignin-Derived Phenols from Biomass Pyrolysis. *Bioresource Technology* **2012**, *124*, 470–477. https://doi.org/10.1016/j.biortech.2012.08.089.

(56) Riazi, M. R. *Characterization and Properties of Petroleum Fractions*; ASTM International: W. Conshohocken, PA, 2005.
(57) Browning, B.; Pitault, I.; Couenne, F.; Jansen, T.; Lacroix, M.; Alvarez, P.; Tayakout-Fayolle, M. Distributed Lump Kinetic Modeling for Slurry Phase Vacuum Residue Hydroconversion. *Chemical Engineering Journal* **2019**, *377*, 119811. https://doi.org/10.1016/j.cej.2018.08.197.